CXCL5 inhibits excessive oxidative stress by regulating white adipocyte differentiation

Dabin Lee [a,b], Kang-Hoon Lee [a], Dong Wook Kim [a], Sanghyuk Yoon [a], Je-Yoel Cho [a,b,*]

[a] Department of Biochemistry, BK21 Plus and Research Institute for Veterinary Science, College of Veterinary Medicine, Seoul National University, Seoul, 08826, Republic of Korea
[b] Comparative Medicine Disease Research Center, Seoul National University, Seoul, 08826, Republic of Korea

ARTICLE INFO

ABSTRACT

Chemokines have been well-documented as a major factor in immune cell migration and the regulation of immune responses. However, recent studies have reported that chemokines have diverse roles, both in immune cells and other cell types, including adipocytes. This study investigated the molecular functions of C-X-C motif chemokine ligand 5 (CXCL5) in white adipose cells using *Cxcl5* knock-out (KO) mice fed a high-fat diet (HFD). The expression of *Cxcl5* decreased by 90% during adipocyte differentiation and remained at a low level in mature adipocytes. Moreover, adipogenesis was enhanced when adipocytes were differentiated from the stromal vascular fraction (SFV) of *Cxcl5* KO mice. Feeding an HFD increased the generation of reactive oxygen species (ROS) and promoted abnormal adipogenesis in *Cxcl5* KO mice. Oxidative stress and insulin resistance occurred in *Cxcl5* KO mice due to decreased antioxidant enzymes and failure to remove ROS. These results indicate the principal roles of CXCL5 in adipogenesis and ROS regulation in adipose tissue, further suggesting that CXCL5 is a valuable chemokine for metabolic disease research.

1. Introduction

In modern populations worldwide, the incidence of metabolic diseases is increasing due to irregular lifestyles and unhealthy eating habits [1,2]. In particular, obesity is a primary driver of many metabolic issues, including inflammation, insulin resistance, Type 2 diabetes, high blood pressure, and cardiovascular disease [3,4]. To better understand and overcome obesity, it is important to study adipose tissues and their differentiation mechanisms.

White adipose tissue (WAT) has been recognized primarily as an organ that stores energy in triglycerides and releases it as free fatty acids. However, current knowledge has expanded the functions of WAT from local energy storage to the secretion of several factors that play a role in several pathophysiological processes, including immune response, hypertension, glucose homeostasis, and cancer. WAT is composed of complex cell types, including adipocytes and immune cells [5]. Cytokines and proteins are secreted mainly from the immune cells surrounding adipocytes to regulate immune responses [6]. In addition, some cytokines, known as adipokines, are secreted by adipocytes and regulate metabolic processes such as food intake, energy homeostasis, adipocyte differentiation, insulin sensitivity, and immune responses. Well-known adipokines include leptin, adiponectin, tumor necrosis factor α (TNFα), and interleukin 6 (IL-6), which are involved in fat metabolism and immune response [7–11].

Chemokines and adipocyte differentiation are an area of active research. A chemokine is a small cytokine that stimulates immune cells' chemical attraction, produced by varied cells in response to infection and other inflammatory stimuli [12]. More than 50 chemokines have been identified in humans and classified into four groups according to the location of preserved cysteine residues (CXCL, CCL, CL, and CX3CL) [12]. In a recent study, CXCL3 and CXCR2 were reported as chemokines and receptors that promote adipocyte differentiation [13,14].

CXCL5 is one of the CXC chemokines secreted by cells when stimulated by inflammatory cytokines such as interleukin 1 (IL-1) and TNFα [15]. CXCL5 stimulates neutrophils and induces an inflammatory response [16]. However, the secretion of CXCL5 in adipocytes and its role is unclear. Here, we generated *Cxcl5* knock-out (KO) mice with the CRISPR/Cas9 system and elucidated the role of CXCL5 in epididymal white adipose tissue (eWAT).

* Corresponding author. Department of Biochemistry, College of Veterinary Medicine Seoul National University, Gwanak-ro1, Gwanak-gu, Seoul, Republic of Korea.
E-mail address: jeycho@snu.ac.kr (J.-Y. Cho).

2. Material and methods

2.1. Animals

Cxcl5 KO mice were generated by deleting exon 1 in the *Cxcl5* gene, as previously described [17]. Mice were maintained under a 12 h light/dark cycle in a controlled-temperature room (22 °C). Five-week-old mice were fed either a 10% normal-fat diet (NFD, control) or a 60% high-fat diet (HFD) (Research diet, USA) for 13 weeks. The Seoul National University Institutional Animal Care and Use Committee (IACUC) approved all animal experiments and protocols (SNU-160825-2-1).

2.2. Adipose Stromal Vascular Fraction (SVF) isolation and adipocyte differentiation

Primary adipocytes were obtained from subcutaneous fat from 4-week-old mice. Subcutaneous fat was minced in collagenase buffer and digested at 37 °C with constant agitation at 160 rpm for 25 min. Digestion was stopped by adding 10 ml serum-containing medium. After filtration through a cell strainer (100 μm), the solution was centrifuged for 5 min at 1,500 rpm, the supernatant was removed, and the pellet was resuspended. Again, cells were filtered through a 40-μm cell strainer and seeded after centrifugation. Isolated preadipocytes were induced to differentiate using MDI media (10% FBS, 0.5 mM IBMX, 1 μM dexamethasone, 10 μg/ml insulin) and 1 μM rosiglitazone. After 2 days, the medium was replaced with a medium containing 10% FBS with 1 μg/ml insulin and changed with 10% FBS media every 2 days. Differentiation of 3T3-L1 preadipocytes was performed following a previous study [17].

2.3. Oil red O staining and triglyceride assay

Differentiated adipocytes were fixed with 10% formalin in PBS for 1 h at room temperature and washed with 60% isopropanol. Cells were stained with Oil Red O solution for 30 min and washed with water. Stained cells were eluted with 100% isopropanol for 10 min, and the absorbance was checked at 500 nm. According to the manufacturer's protocol, the triglyceride level was measured using a Triglyceride Quantification Kit (BM-TGR-100, BIOMAX, KR).

2.4. Reactive Oxygen Species (ROS) measurement

ROS production was induced by treatment with 200 or 300 μM of H_2O_2. for 24 h. The level of intracellular ROS was measured via cell-permeant 2',7'–dichlorofluorescein diacetate (H₂DCFDA) staining.

Green fluorescence was detected by microscopy (ECHO, US). To increase the accuracy of the data, pictures were taken at random. And all pictures were analyzed for fluorescence intensity using ImageJ software (Fiji ImageJ).

2.5. LC-MS/MS analysis

eWAT was dissected from wild-type (WT), and *Cxcl5* KO mice fed an HFD for 13 weeks, and total protein was extracted from the tissues. The proteins were digested with trypsin. Digested peptides were labeled with isobaric tags for relative and absolute quantitation (iTRAQ) (AB Sciex, Framingham, MA) to normalize protein amounts quantitatively. Then, anion exchange-based fractionation was performed to identify more proteins. The fractionation was performed by following the protocol by Matthias et al. [18]. LC-MS/MS analysis was performed with Q Exactive (0726090, Thermo Scientific, US). Using the raw data obtained after LC-MS/MS analysis, proteins were identified with MaxQuant (version 1.5.8.3) and normalized with Scaffold Q+ software (Scaffold 4.7.5; Proteome Software, Portland, OR).

2.6. RNA isolation and quantitative RT-PCR

Total RNA was isolated with TRIzol (15596018, Ambion, US) from cells or tissues, and reverse transcription was performed using Omniscript (205113, QIAGEN, DE) according to the manufacturer's protocol. SYBR green (S7563, Invitrogen, US) and GO Taq (M8298, Promega, US) were used for quantitative real-time PCR with specific primers (listed in Table S1). The expression of all target genes was normalized with *36b4*.

2.7. Western blot and histological analysis

Proteins were extracted using 4% SDS Tris/HCl pH lysis buffer for tissue samples and RIPA buffer for cells (89900, Thermo Scientific, US). Tissue samples were homogenized before lysis at 100 °C, and clear supernatant was obtained by centrifugation for further use. Cells were lysed in RIPA buffer by incubation for 30 min on ice followed by sonication. After that, the lysate was centrifuged for 10 min at 14,000 rpm. Western blot protocol was performed as detailed previously paper [17] to detect the expression of PPARγ (2430, Cell signaling, US), PRDX4 (P3352-25L, BIOMOL, DE), p-AKT (9271S, Cell signaling, US), Total AKT (9272, Cell signaling, US), p-JNK (9255S, Cell signaling, US), Total JNK (9252S, Cell signaling, US), and α-tubulin (LF-MA0117, AB Frontier, KR). Histological analysis was performed following previous studies [17].

2.8. Luciferase assay

HEK293T cells were plated on 24-well plates at a density of 50–60% confluence and transiently transfected with PPARα, retinoid X receptor α [RXRα], β-galactosidase, and DR-1 DNA plasmid by the lipofectamine 3000 (L3000001, Thermo Scientific, US) according to the manufacturer's protocol. Forty-four hours after transfection, the cells were treated with rosiglitazone, alone or with recombinant CXCL5, for 24 h. The transcription efficiency of the reporter gene was confirmed through luciferase activity normalized to β-galactosidase activity.

2.9. Intraperitoneal Glucose Tolerance Test (IPGTT)

Mice fasted for 16 h before intraperitoneal (i.p.) injection with 2.0 g/kg glucose. Approximately 20 μl of blood was collected from the mice at 0, 15, 30, 60, 90, and 120 min after glucose injection, and blood glucose was measured using an Accu-check Performa glucometer (Roche).

2.10. Thiobarbituric Acid Reactive Substance (TBARS) assay and cholesterol assay

A TBARS assay was performed using a TBARS Assay Kit (BO-TBR-200, BIOMAX, KR) to measure the level of lipid peroxidation in the adipose tissue of the mice fed an HFD. Both esterified and unesterified cholesterol (free cholesterol) were measured in serum using a Total cholesterol assay kit (BM-CHO-100, BIOMAX, KR). Both analyses were performed according to the manufacturer's protocols.

2.11. Statistical analysis

All analyses were performed with Graph Pad Prism 7 software, and the data were expressed as means ± standard error of the mean (SEM). Statistical analysis was performed using the unpaired two-tailed Student's t-test to compare multiple variables. Significance was defined as $*p < 0.05$, $**p < 0.01$, $***p < 0.001$ and $****p < 0.0001$.

3. Results

3.1. Proteomic analysis revealed that the function of Cxcl5 in adipocytes reversely associates with fatty acid metabolic process including oxidation-reduction

We performed a proteomic analysis of epididymal white adipose tissue (eWAT) obtained from WT and *Cxcl5* KO mice to explore the roles of the chemokines expressed in adipocytes. The eWAT was isolated from 18-week-old WT and *Cxcl5* KO mice, and the tissue was prepared for proteomics analysis (Fig. 1A). A total of 1,765 proteins were identified; differentially expressed proteins (DEPs) are represented by the heatmap and volcano plot in Fig. 1B and C. A total of 136 proteins were significantly different (66 upregulation and 70 downregulation) in *Cxcl5* KO compared with WT mice (Tables S2 and 3). The up-and downregulated DEPs were subjected to gene ontology (GO) and network enrichment analyses separately. The terms enriched in upregulated DEPs suggested that many proteins are functionally associated with actin filament organization, fragmentation, and actin-binding; these functions determine cell shape, nuclear shape, cell spreading, and cell stiffness affect cell differentiation (Fig. 1D and E). Interestingly in the enrichment analysis, serum response factor (SRF) was enriched in the upregulated proteins of *Cxcl5* KO, as confirmed in the transcription factor-target interaction database for humans and mice in TRRUST (transcriptional regulatory relationships unraveled by sentence-based text mining) (Fig. 1F). It is well known that SRF induces actin cytoskeleton organization together with myocardin-related transcription factor A (MRTFA), a co-activator of SRF [19] and that it inhibits brown fat or beige fat differentiation [20,21]. The DEPs downregulated in *Cxcl5* KO were enriched in lipid

metabolism and oxidoreductase (Fig. 1G and H). It is meaningful for the clinical approach because the proteins related to fat metabolism, including cholesterol transport and metabolism, were decreased (Fig. 1H). Proteins downregulated in *Cxcl5* KO eWAT were associated with PPARγ and SREBP1 transcription factors in TRRUST database (Fig. 1I). Since PPARγ and SREBP1 are essential transcription factors for the differentiation of white adipocytes, it is postulated that *Cxcl5* could influence the differentiation of adipocytes.

3.2. Depletion of Cxcl5 enhances adipogenesis

We thus confirmed the role of *Cxcl5* in adipocyte differentiation. Since Kabir et al. previously reported on the expression of chemokines during adipogenesis [9], the changes in *Cxcl5* expression were examined during the differentiation of 3T3-L1 cells into adipocytes. Adipocyte maturation was measured by the accumulation of lipid droplets and changes in the expression of marker genes such as *Pparγ* (proliferator-activated receptor-gamma), *C/ebp* (CCAAT-enhancer-binding protein), and *Glut4* (glucose transporter type 4) (Fig. 2A and B). During differentiation, *Cxcr2* expression dramatically increased beginning on induction day 4, while the expression of its ligands, such as *Cxcl1, Cxcl3,* and *Cxcl5,* varied (Fig. 2C). *Cxcl2* was not detected during differentiation, and *Cxcl3* expression increased, while *Cxcl1* and *Cxcl5* decreased during adipogenesis. Notably, although the expression of *Cxcl5* decreased by more than 90% beginning early in the process (Day 2), the roles of *Cxcl5* in the differentiation of adipocytes are still unclear.

We then examined the effect of *Cxcl5* depletion on adipocyte differentiation using *Cxcl5* KO mice. A stromal vascular fraction (SVF) was isolated from the WAT of both WT and *Cxcl5* KO mice to differentiate into adipocytes (Fig. 2D). Interestingly, significant increases were found in the number of matured adipocytes and the deposits of lipid and fat in *Cxcl5* KO (Fig. 2E). This observation was also validated by the higher absorbance of the cells stained with Oil Red O (Fig. 2F) and the higher triglyceride concentration in *Cxcl5* KO (Fig. 2G). Most of all, significant increases in the expression of adipogenesis marker genes such as *Pparγ, Fas* (fatty acid synthase), *Serbp1-c* (sterol regulatory element-binding protein 1-c), *Acaca* (acetyl-CoA carboxylase alpha), *Nox4* (NADPH Oxidase 4), and *Adipoq* (adiponectin) in *Cxcl5* KO indicated that *Cxcl5* deficiency enhances adipogenesis. Except for *Nox4*, all other markers were significantly up-regulated in *Cxcl5* KO mice in the early sage of differentiation SVF (Fig. 2H). It is of note that the marker genes were decreased thereafter, because adipose tissue is mainly composed of mature adipocytes after rapid differentiation. Typically, the difference in gene expression between WT and *Cxcl5* KO was largest after six days of differentiation (Fig. 2G). PPARγ protein levels were also significantly up-regulated in adipocyte differentiation of *Cxcl5* KO (Fig. 2I). These results strongly suggest that *Cxcl5* negatively regulates adipocyte differentiation.

3.3. CXCL5 treatment inhibits adipogenesis

We hence conducted an experiment to introduce recombinant CXCL5 to clarify the relationship between CXCL5 and adipogenesis. 3T3-L1 cells were treated with recombinant CXCL5 during adipocyte differentiation for 6 days. As expected, it was confirmed that abundant CXCL5 inhibited the differentiation of preadipocytes into adipocytes. The decreases in lipid droplets in cells and the absorbance value for Oil red O staining in the recombinant CXCL5 treated group demonstrated that CXCL5 is negatively associated with adipogenesis (Fig. 3A and B). Also, the triglycerides level was lower in adipocytes treated with recombinant CXCL5 than in control (Fig. 3C). The adipogenesis-associated genes *Pparγ, Srebp1-c,* and *Glut4* were significantly down-regulated by CXCL5 treatment during adipocyte differentiation (Fig. 3D). It was demonstrated that CXCL5 negatively affects adipocyte differentiation, we then tested whether CXCL5 regulates PPARγ, a master regulator in adipocyte differentiation. A luciferase reporter assay of the transcriptional activity
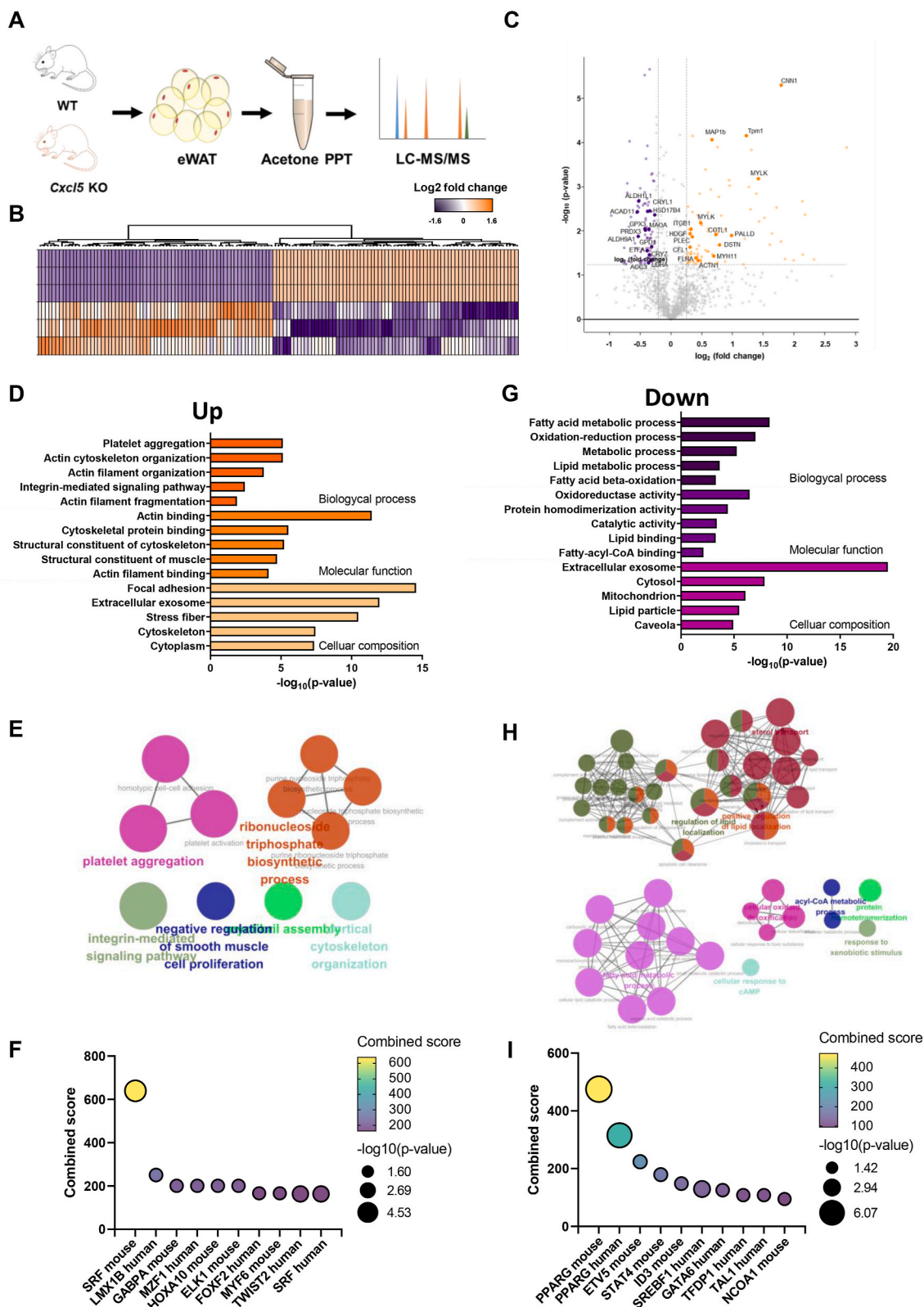
Fig. 1. Adipogenesis was high but the expression of lipid metabolism-related proteins was low in *Cxcl5* KO mice. A) Schematic diagram of proteomics analysis using eWAT from WT and *Cxcl5* KO mice. B) Heatmap and C) volcano plots of proteins with a more than 1.2-fold increase (orange) or decrease (purple) in *Cxcl5* KO mice. GO analysis of proteins (top 5) differentially expressed in the eWAT of *Cxcl5* KO mice. GO analysis results of D) upregulated and G) downregulated proteins. The Network between GO terms in DEP with E) upregulated and H) downregulated eWAT in *Cxcl5* KO mice. Enrichr analysis results from TRRUST transcription factors 2019 database for transcription factors of F) upregulated and I) downregulated proteins in *Cxcl5* KO mice. (For interpretation of the references to colour in this figure legend, the reader is referred to the Web version of this article.)
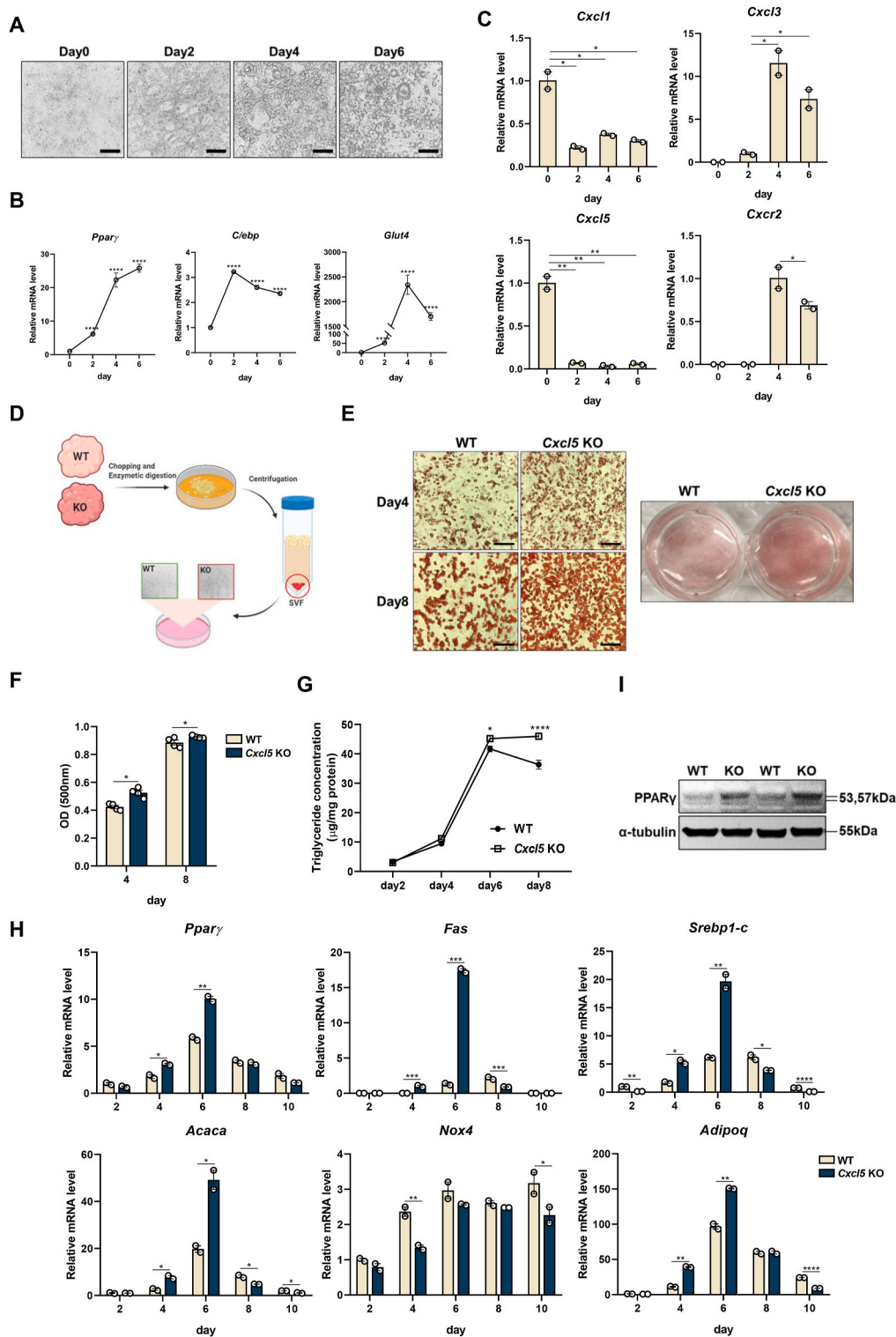
Fig. 2. *Cxcl5* mRNA expression is dramatically downregulated during adipogenesis. A) 3T3-L1 adipocytes were differentiated by treatment with MDI (0.5 mM 3-isobutyl-1-methylxanthine, 1 μM dexamethasone, and 10 μg/mL insulin) for 2 days. Next, after incubation for the next 2 days in a medium containing insulin, the medium was replaced with Dulbecco's modified eagles medium (DMEM) medium and exchanged once every two days until differentiation was complete. B) mRNA expression of the adipogenic marker gene. C) Changes in mRNA expression of *Cxcr2* and its ligands during the differentiation of adipocytes. D) Schematic diagram of the separation of SVF from adipose tissue. E) Differentiation of SVF isolated from WT and *Cxcl5* KO mice into adipocytes was confirmed by Oil red O staining. Scale bar = 200 μm. F) Stained cells were dissolved with isopropanol, and the OD measured at 500 nm. G) Triglyceride concentrations of WT and *Cxcl5* KO during adipocyte differentiation. H) Expression of adipogenic gene mRNA in WT and *Cxcl5* KO during adipocyte differentiation. After adipocyte induction I) PPARγ protein expression levels in WT and *Cxcl5* KO. Statistical analysis was performed using two-tailed unpaired Student's t-tests. *$p < 0.05$, **$p < 0.01$ and ***$p < 0.001$. (For interpretation of the references to colour in this figure legend, the reader is referred to the Web version of this article.)
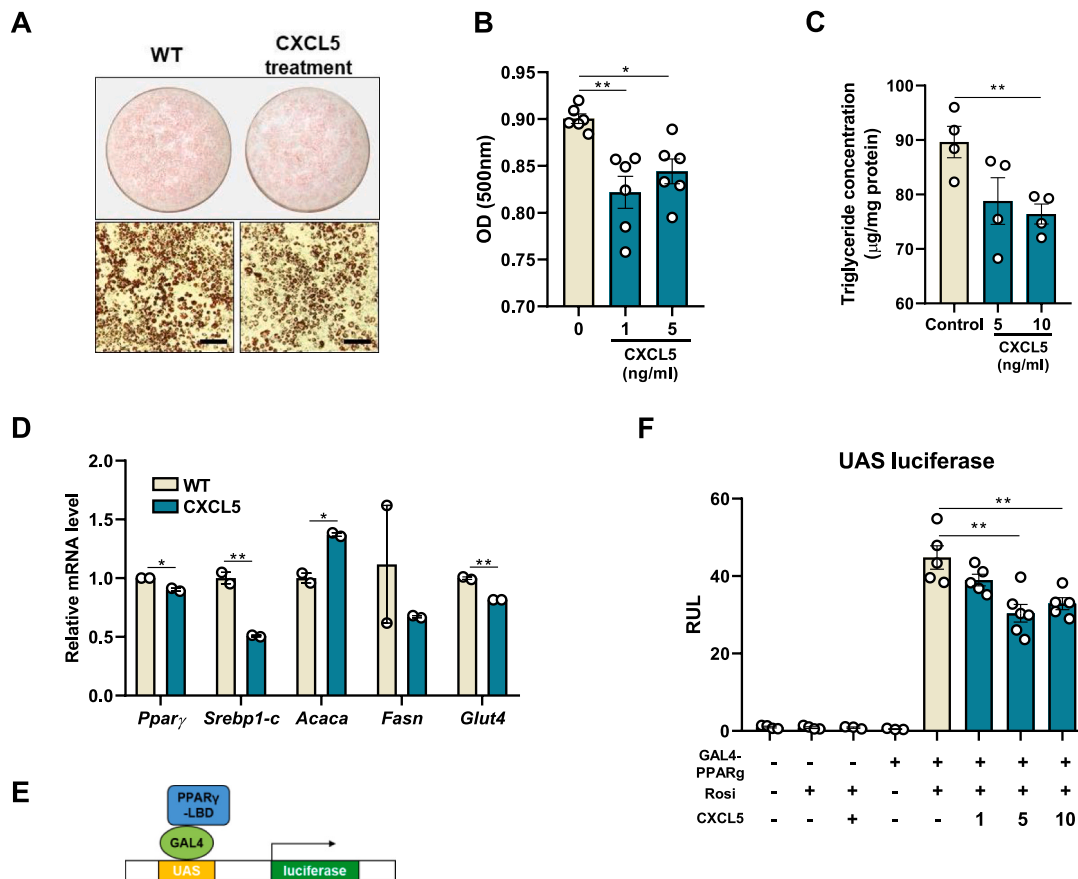
Fig. 3. Treatment with CXCL5 inhibits adipocyte differentiation by decreasing the transcriptional activity of PPARγ. A) During the differentiation process, 3T3-L1 cells were treated with MDI and recombinant CXCL5 to induce differentiation and stained with Oil red O. Scale bar = 200 μm. B) OD level of Oil red O staining. C) Triglyceride levels and D) mRNA expression levels of adipogenesis markers after the induction of adipocyte differentiation via treatment with recombinant CXCL5. Effect of CXCL5 on UAS luciferase reporter activity with Gal4-PPAR-LBD in HEK293T cells (n = 6) E) Schematic diagram for UAS luciferase assay system F) Treatment of rosiglitazone (1 μM) with or without recombinant CXCL5 Statistical analysis was performed using two-tailed unpaired Student's t-tests. *$p < 0.05$ and **$p < 0.01$. (For interpretation of the references to colour in this figure legend, the reader is referred to the Web version of this article.)

of PPARγ was induced via treatment with rosiglitazone, the ligand of PPARγ, alone or with recombinant CXCL5 (Fig. 3E). Luciferase activity was inversely related to the amount of CXCL5 used to treat the cells (Fig. 3F). These results suggest that CXCL5 inhibits the transcriptional activity of PPARγ in a ligand-binding, domain-dependent manner. Our data strongly indicate that CXCL5 negatively regulates the differentiation of adipocytes.

3.4. Adipocytes differentiated from Cxcl5 KO mice have high ROS

Since numbers of GO terms associated with fatty acid or lipid metabolism, including oxidation-reduction, and a fatty acid β-oxidation, were enriched in the down-regulated DEP of Cxcl5 KO (Fig. 1F) and a solid association has been reported between excessive fat accumulation and high production of ROS [22], we measured the amount of ROS in both Cxcl5 KO and WT. H2DCFDA staining showed that the basal level of intracellular ROS was higher in Cxcl5 KO than in WT (Fig. 4A). We also measured the transcription levels of antioxidant genes such as the Prdx (peroxiredoxin) gene group, Sod1 (superoxide dismutase), Cat (catalase), and Gpx3 (glutathione peroxidase3). Of note, several antioxidant genes were increased in Cxcl5 KO compared to WT at the beginning of differentiation and dramatically downregulated at the end of differentiation (Fig. S1). Furthermore, in the oxidative stress condition of exposure to H2O2, ROS accumulation increased robustly in Cxcl5 KO cells. H2DCFDA stained the most brightly on the Cxcl5 KO cells upon exposure to H2O2 (Fig. 4A). It was confirmed again in the gene

expression levels of antioxidant enzymes. As shown in Fig. S1, most antioxidant enzymes, including Prdx1, decreased at the transcription level in Cxcl5 KO. H2O2 induced significant increases in the expression of some of these enzymes, such as MnSod, in WT but not in Cxcl5 KO (Fig. 4C). Most of the genes, including Prdx2,3,4,5, Sod1, Cat, and Nrf2, were maintained or slightly increased when WT adipocytes were treated with H2O2, but they were still expressed at low levels in Cxcl5 KO adipocytes. Western blots of representative proteins PRDX4 and MnSOD show that the antioxidant enzymes downregulated in Cxcl5 KO are less responsive to H2O2 than in WT adipocytes (Fig. 4B).

Conversely, the generation of ROS and the expression of antioxidant enzymes were confirmed when adipogenesis while treated with CXCL5. As a result, ROS production was decreased when differentiated while treated with CXCL5 (Fig. 4D and E), but there was no difference in the expression of antioxidant enzymes (Fig. 4F). On the other hand, we also tested if reducing ROS during adipogenesis can restore normal adipogenesis in Cxcl5 KO by antioxidant treatment (Fig. S2). Expectedly, antioxidants treatment retarded or blocked adipogenesis in a concentration-dependent manner. Since ROS effects on adipogenesis were too obvious to hypothesize that Cxcl5 directly regulates antioxidant enzyme expression, we thus propose that Cxcl5 depletion promotes the differentiation of adipocytes, resulting in substantial ROS accumulation that induces chronic oxidative stress.
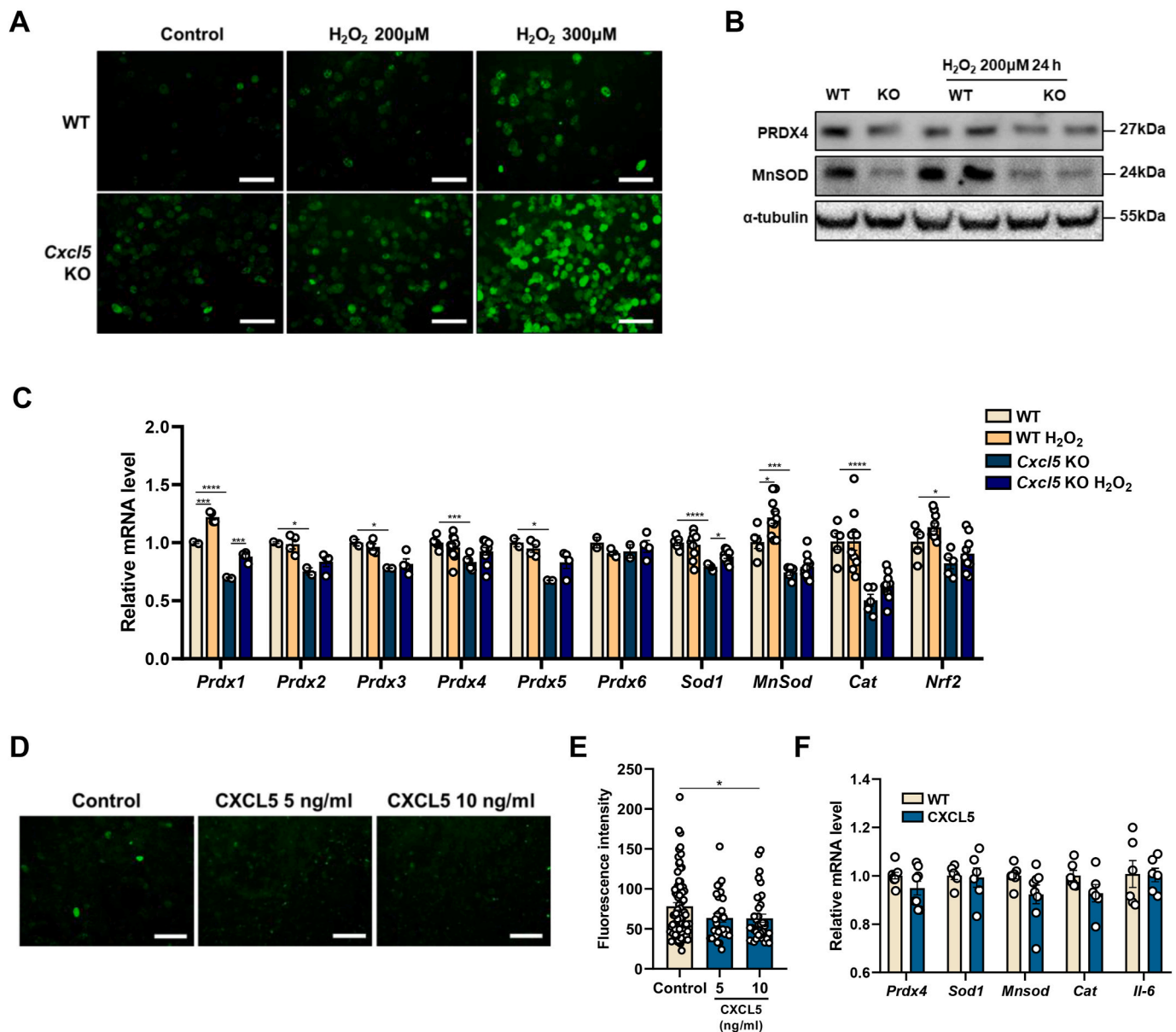
Fig. 4. Adipocytes differentiated from *Cxcl5* KO mice have high ROS. A) ROS measurement in adipocytes of WT and *Cxcl5* KO mice and after 200 or 300 μM H$_2$O$_2$ treatment in adipocytes of WT and *Cxcl5* KO mice. B) PRDX4 and MnSOD expression measured by Western blot and C) mRNA expression of antioxidant enzyme after H$_2$O$_2$ treatment in adipocytes of WT and *Cxcl5* KO mice. D) ROS measurement in 3T3-L1 adipocytes differentiated with recombinant CXCL5. E) Quantification of green fluorescence signal in the 3T3-L1 adipocytes. F) mRNA expression of antioxidant enzyme in 3T3-L1 adipocytes with or without recombinant CXCL5. Statistical analysis was performed using two-tailed unpaired Student's t-tests. *$p < 0.05$ and **$p < 0.01$. (For interpretation of the references to colour in this figure legend, the reader is referred to the Web version of this article.)

3.5. HFD amplified the systemic oxidative stress caused by impaired antioxidant enzymes in Cxcl5 KO mice

Since our results showed that CXCL5 is strongly associated with a high level of ROS and fat metabolism in adipocyte tissue, we fed a HFD to *Cxcl5* KO mice for 13 weeks (Fig. 5A). Based on the previous results, we hypothesized that *Cxcl5* KO mice fed with HFD would exhibit the disturbance of ROS scavenging or oxidative-stress-related proteins and thus an increased oxidative stress condition. Fig. 5A illustrates the scheme of the experiment. After eWAT tissue sampling, the proteins were digested by the in-solution digestion method. Digested peptides were labeled with iTRAQ to normalize protein amounts quantitatively. After labeling the fragmented peptides with the iTRAQ isobaric mass tags, the sample was fractionated into six by anion exchange

fractionation. After that, mass spectrometry was performed to obtain comparative proteome quantitation. A total of 1,781 proteins was identified in the eWAT (Table S4). To understand the role of CXCL5 in HFD-mediated ROS, we sorted out the proteins that were upregulated in WT HFD but not in the NFD or *Cxcl5* KO HFD groups (Fig. 5B). A total of 324 proteins were retrieved and subjected to GO analysis. We found that the protein reduced in *Cxcl5* KO was enriched with proteins involved in responses to oxidative stress and cellular redox homeostasis, consisting of antioxidant proteins that scavenge ROS (Fig. 5C and Table 1). The data show that the eWAT of *Cxcl5* KO fed HFD poorly expresses the antioxidant proteins and thus has increased ROS with a more severe oxidative stress condition.

To validate the proteome analysis, we first measured the level of oxidative stress through lipid peroxidation in the eWAT that was
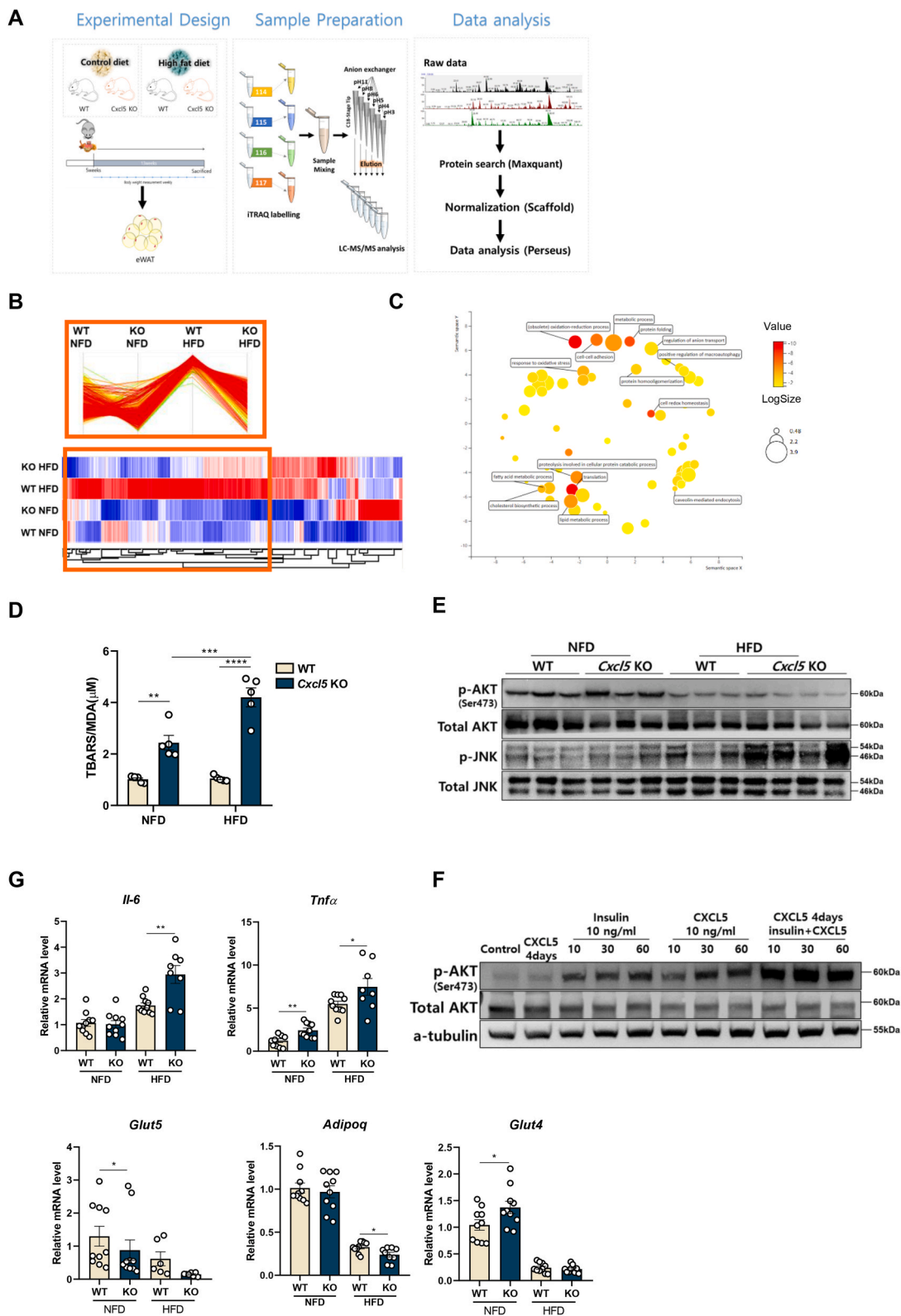
Fig. 5. Increased oxidative stress due to decreased antioxidant proteins in *Cxcl5* KO mice A) Schematic diagram of proteomic analysis of WT and *Cxcl5* KO mice fed an NFD or HFD. B) Heatmap with a pattern that increases in WT HFD but decreases in *Cxcl5* KO HFD. and C) GO analysis of proteins that decreased in *Cxcl5* KO HFD eWAT among the list of proteins increased more than 1.2 times in WT HFD eWAT compared to WT eWAT. D) Lipid peroxidation evaluated by the TBARS assay in eWAT of WT or *Cxcl5* KO mice fed NFD and HFD. E) Western blot of phosphorylation AKT ^{Ser473} and phosphorylation JNK in eWAT proteins from WT or *Cxcl5* KO mice fed NFD and HFD. F) Western blot of phosphorylation AKT ^{Ser473} and total AKT in 3T3-L1 cells treated with CXCL5 or insulin or treated together. G) mRNA expression of *Il-6*, *Tnfα*, *Adipoq*, *Glut4*, and *Glut5*. The *36b4* gene was used for internal controls for RNA and protein. Statistical analysis was performed using two-tailed unpaired Student's t-tests. *$p < 0.05$ and **$p < 0.01$.

Table 1
List of reduced antioxidant enzymes in Cxcl5 KO mice fed a high-fat diet.

Official gene symbol	Gene name	Difference
DLD	dihydrolipoamide dehydrogenase	2.502939
PRDX1	peroxiredoxin 1	1.626282
PRDX2	peroxiredoxin 2	1.621552
PRDX3	peroxiredoxin 3	1.780662
PRDX4	peroxiredoxin 4	3.837177
PRDX5	peroxiredoxin 5	2.43681
PRDX6	peroxiredoxin 6	1.647107
P4HB	prolyl 4-hydroxylase, beta polypeptide	2.236035
PDIA3	protein disulfide isomerase associated 3	1.634867
PDIA4	protein disulfide isomerase associated 4	1.612836
PDIA6	protein disulfide isomerase associated 6	1.541046
TXNDC5	thioredoxin domain containing 5	1.615277
TXNL1	thioredoxin-like 1	2.829663

obtained from WT or *Cxcl5* KO mice fed an NFD or HFD. Lipid peroxidation was evaluated using TBARS, a ROS indicator. It was confirmed that TBARS was higher in *Cxcl5* KO **mice** regardless of diet (Fig. 5D). Since previous studies have reported that the accumulation of intracellular ROS increases the phosphorylated JNK signal and decreases phosphorylated AKT [23,24], we thus examined these two signaling pathways in WT and *Cxcl5* KO **mice with** different diet conditions. The data clearly showed that phosphorylated AKT ^{Ser473} decreased and phosphorylated JNK increased in the eWAT of *Cxcl5* KO, and the difference was more significant in the HFD groups (Fig. 5E). In addition, when CXCL5 was treated with insulin in 3T3-L1 cells, p-Akt^{Ser473} signaling was further activated than insulin alone (Fig. 5F). Together these data indicate that CXCL5 have a positive effect on ROS and insulin signaling regulation. Furthermore, the expression of inflammation markers such as *Tnfα* and *Il-6* was higher in the eWAT of *Cxcl5* KO, while *Adipoq* expression was lower (Fig. 5G). These results suggest that the accumulation of ROS in the *Cxcl5* KO mice fed an HFD due to their impaired antioxidant enzyme activities results in the increased inflammatory response in the eWAT.

3.6. HFD combined with Cxcl5 deficiency increased insulin resistance and cholesterol in the blood

Since all of the results indicated that *Cxcl5* deficiency may cause functional damage in eWAT, we characterized *Cxcl5* KO mice regarding metabolic-related phenotypes. Unexpectedly, a significant difference in body weight was observed between the *Cxcl5* KO and WT groups fed an HFD, but lean and fat mass/body weight, free body fluid, and amount of eWAT tissue weight/body weight (TW/BW) did not significantly differ (Fig. 6A–C). Also, there was no significant difference in histology between WT and *Cxcl5* KO mice fed an NFD. However, distinct differences in histology were observed in the groups fed a HFD; *Cxcl5* KO mice fed an HFD exhibited larger adipocytes than WT mice fed a HFD (Fig. 6D). Accurate measurements of the size of the adipocytes confirmed that the adipocytes were significantly larger in *Cxcl5* KO mice fed an HFD (Fig. 6E). In particular, the numbers of macrophages that penetrated the adipose tissue and stained crown-like structures were significantly higher (Fig. 6E). We also performed a histological analysis of other adipocyte tissues (inguinal white adipose tissue (iWAT), brown adipose tissue (BAT)), and the liver. As in the eWAT, the adipocytes were enlarged in *Cxcl5* KO mice fed an HFD (Figs. S3A and B). Moreover, a fatty liver was found in *Cxcl5* KO mice, and it became severe in the *Cxcl5* KO group fed an HFD (Fig. S3C). Fat accumulation was confirmed in the liver of *Cxcl5* KO mice, and when the expression levels of *Irs1,2* and *Glut4* in the liver were checked, they were not significantly different from those of the WT HFD group (Fig. S4). The blood glucose level was higher in *Cxcl5* KO than in WT in the groups fed an NFD (Fig. 6F), and in the intraperitoneal glucose tolerance tests, blood glucose levels were significantly higher in the *Cxcl5* KO mice fed an HFD (Fig. 6G). These results suggest that oxidative stress caused by *Cxcl5* deficiency triggers

insulin resistance. In addition, consistent with previous findings that ROS induces intracellular lipid accumulation and causes an increase in cholesterol [25], total cholesterol level was significantly higher in *Cxcl5* KO than in WT mice when feeding either an NFD or an HFD. Cholesterol presents in the body in two different forms: esterified cholesterol and free cholesterol. However, only free cholesterol is biologically active and has cytotoxicity [26], so the concentration of free cholesterol was measured separately. Notably, the free cholesterol level was significantly higher in *Cxcl5* KO mice regardless of diet (Fig. 6H). Altogether, the increase in ROS and decrease in antioxidant proteins caused by *Cxcl5* deficiency induces insulin resistance and increases cholesterol in the body, suggesting that fat metabolism and the metabolic system in the body were damaged in *Cxcl5* KO mice.

4. Discussion

The adipose tissue in the body is a vital organ that stores extra energy. However, improper enzyme functions in this tissue cause excessive lipid accumulation, resulting in various metabolic diseases. Thus, proper differentiation of adipocytes and accumulation and decomposition of fat help maintain energy homeostasis in the body [27]. Recent studies, including ours, have suggested the involvement of *Cxcl5* in adipogenesis and lipid metabolism [17]. CXCL5 is known as a chemokine secreted in inflammatory diseases and is highly expressed in metabolic diseases. For example, CXCL5 is highly expressed in obese or diabetic patients and is associated with hypercholesterolemia. It has been reported that the in vivo concentration of CXCL5 is abnormally higher than physiological concentrations in patients with these diseases [28–30]. Conversely, we have previously reported that CXCL5 is required for normal lipid metabolism and that UCP1 is less expressed in *Cxcl5* KO **individuals** under cold stress conditions [17]. As such, there is still confusion regarding the role of CXCL5, but in this study, we describe CXCL5 as a factor regulating healthy differentiation in adipocytes. Our results seem contradictory to the previous study that CXCL5 promotes insulin resistance [28], but there are differences between the two studies. First, there is a big difference in the target cell type expressing CXCL5. The previous study focused on the M1 macrophage, but the current study on adipocytes. Second, experimental conditions are different. This study focused on the adipocyte differentiation condition instead of inflammatory condition that was tested in the previous study. Third, from the adipogenesis point of view, the previous study looked at the adipose tissue, which means that differentiation was already done, and the CXCL5 level would be low. On the contrary, the current study focused on the role of Cxcl5 in the early stage of adipocyte differentiation using the *Cxcl5* KO mice. The cells have low *Cxcl5* levels, and adipocyte differentiation was not occurring appropriately.

This study suggests that CXCL5 is involved in adipocyte differentiation and expansion and consequently regulates antioxidant enzymes. Our data confirmed that pre-adipocytes differentiation into mature adipocytes was increased in *Cxcl5* KO mice (Fig. 1). *Cxcl5* expression must be downregulated for healthy differentiation of adipocytes. Contrary to the well-known inflammatory response of CXCL5, during the normal differentiation of adipogenesis, CXCL5 might not participate in the inflammatory response. The role of CXCL5 that we have identified is to induce the healthy differentiation of adipocytes. As shown in Fig. 2, the expression of various chemokines and their receptors is regulated during adipocyte differentiation. When adipocyte differentiation occurs, *Cxcl1* or *Cxcl5* decreases, but the expression of *Cxcl3* or *Cxcr2* increases. These results are consistent with studies showing that *Cxcl3* and *Cxcr2* induce adipogenesis [13,14]. Conversely, *Cxcl5*, which was reduced during adipocyte differentiation, inhibited the differentiation in our data. Accordingly, if we focused on the end stage of adipocyte differentiation or fully differentiated adipocyte, transgenic mice overexpressing *Cxcl5* can be a better mouse model than the *Cxcl5* KO mice model. However, we think that the *Cxcl5* KO mice model is better since we looked at an early stage of adipogenesis. Moreover, we also conducted the
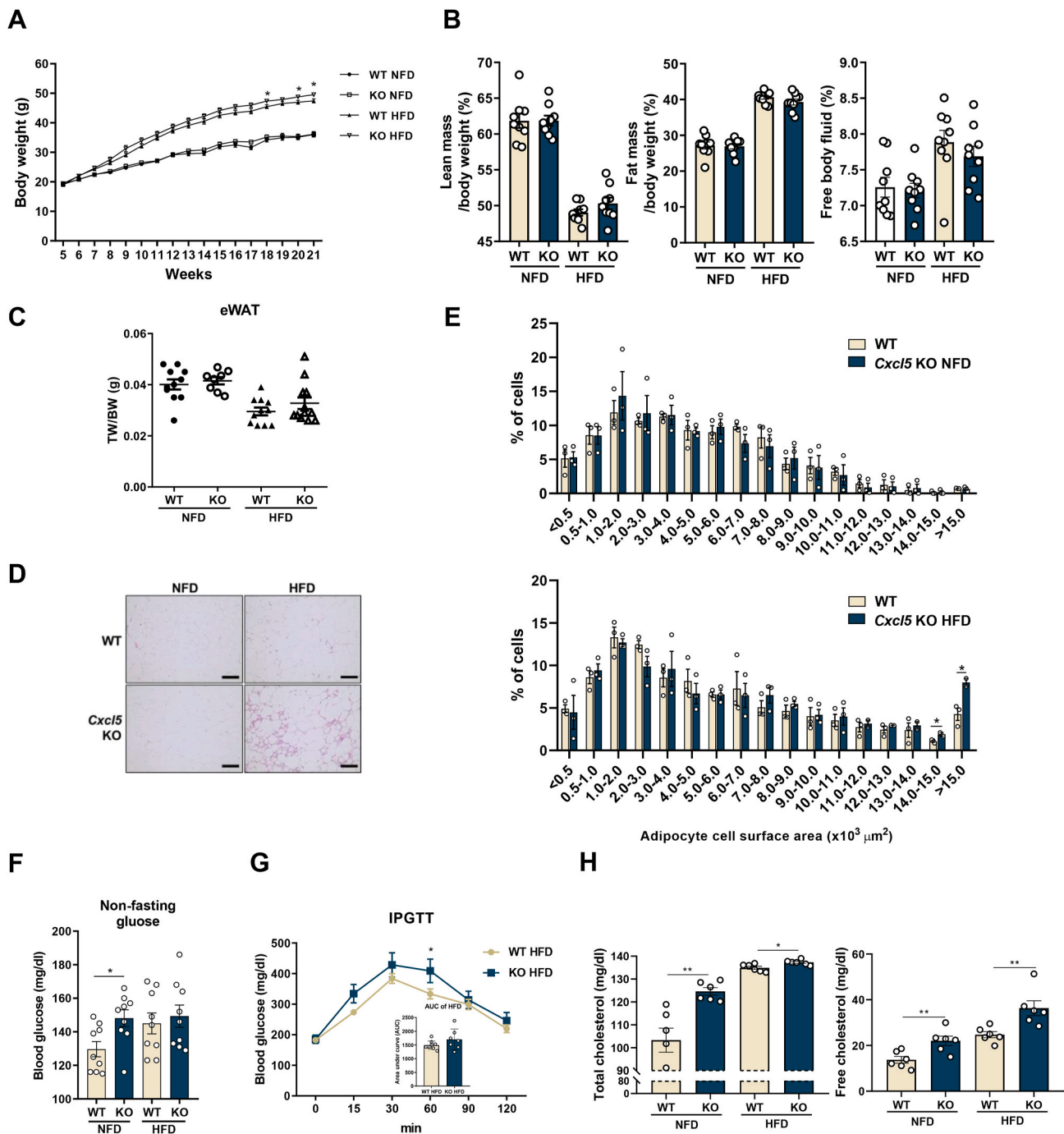
Fig. 6. Increased insulin resistance and cholesterol due to fat accumulation during irregular regional differentiation in *Cxcl5* KO mice. A) Graphs of body weight gain when fed an NFD or HFD for 16 weeks. B) Body composition of WT and *Cxcl5* KO mice fed an NFD or HFD. Representative images of C) weight of eWAT/body weight and D) eWAT H&E staining of WT and *Cxcl5* KO mice fed an NFD or HFD. Scale bar = 200 μm. E) The diameter of the lipid droplet in H&E staining of eWAT. F) Non-fasting blood glucose levels in WT and *Cxcl5* KO mice fed an NFD or HFD. G) Intraperitoneal glucose tolerance test (IPGTT) results for WT and *Cxcl5* KO mice fed an HFD for 16 weeks. (n = 8) IPGTT measurement was performed for up to 120 min by injecting 2 g glucose/kg body weight into the fasting mouse for 16 h. H) Determination of total and free cholesterol in the serum of mice fed an NFD or HFD. Statistical analysis was performed using two-tailed unpaired Student's t-tests. $*p < 0.05$ and $**p < 0.01$.

overexpression experiment by treating the recombinant CXCL5 protein, and successfully showed that CXCL5 inhibits adipocyte differentiation. In *Cxcl5* KO cells, differentiation markers are expressed very highly compared to WT in the early stage of differentiation, and show a decreasing pattern in the late stage of differentiation (Fig. 2H). At the end of differentiation, a decrease in adiponectin, a hormone that helps metabolism and a differentiation marker, was confirmed. It was not only at the cellular level but also in the *Cxcl5* KO eWAT tissue (Fig. 5G).

Eventually, in *Cxcl5* KO, differentiation occurs rapidly, and a lot and adipose tissue is abnormally formed which is considered to eventually show an insulin resistance phenotype. Additionally, we suggested the mechanism of CXCL5 in the regulation of adipogenesis related gene expression via PPARγ. There were two possible ways in which CXCL5 could regulate PPARγ function. We first showed that PPARγ expression was increased in *Cxcl5* KO. The other finding was that treatment with CXCL5 inhibits the transcriptional activity of PPARγ via the influence of

the ligand-binding domain. Further study of the molecular functions of CXCL5 regarding its influence on PPARγ activity will be guaranteed.

Numerous antioxidants function to remove ROS in the body [31]. Changes in antioxidant enzymes have several implications. When ROS is low, the expression of antioxidant enzymes is low. Conversely, when ROS is too high and intracellular regulation is impossible, the expression of antioxidant enzymes may be low [32]. Impaired adipogenesis in *Cxcl5* KO triggers ROS accumulation, leading to oxidative stress in adipocytes (Fig. 4A). As a result, it also fails to regulate the expression of antioxidant enzymes (Fig. 4B, C, Fig. S1). As a feedback action, adipocytes from *Cxcl5* KO mice were better differentiated with more ROS accumulation than adipocytes from WT mice (Figs. 2E and 4A). As a consequence of the above functions, *Cxcl5* deficiency led to inflammatory reactions and insulin resistance in *Cxcl5* KO mice. Although there is no significant difference in the weight or weight of fat, there are many other values and features that should be considered for abnormalities in adipocytes and adipogenesis. We showed that the overall glucose concentration was not properly regulated in the *Cxcl5* KO HFD group in IPGTT data and confirmed that the ROS was high and crown-like structures were more visible in the eWAT fed *Cxcl5* KO HFD; these were found not only in eWAT but also in BAT and the liver (Fig. S3). It is meaningful because oxidative stress in the liver is a crucial mechanism in developing non-alcoholic fatty liver disease [33]. These characteristics were more severe in the *Cxcl5* KO group fed an HFD because *Cxcl5* deficiency makes it more challenging to regulate ROS, so it is expected that fatty liver formation is severe in *Cxcl5* KO. These results suggest that it is worth studying the relationship between the mechanisms of CXCL5 and the fatty liver. ROS increases during metabolism even in brown adipose tissue, but in *Cxcl5* KO mice, ROS increases further, and the lipid droplets of BAT become larger, as seen in eWAT. ROS is regulated by UCP1, which is highly expressed in BAT [34], and it is expected that ROS might not be properly regulated in *Cxcl5* KO due to the decrease of UCP1 [17]. Lastly, free cholesterol and total cholesterol were the highest in *Cxcl5* KO HFD.

The current study strongly suggests that ROS accomplished more active adipocyte differentiation in *Cxcl5* KO cells. Previous studies have shown that, among many other factors, ROS promotes adipocyte differentiation [22,35]. Since too much ROS accumulation will eventually damage the cells, more studies are required to determine the levels of ROS needed for better differentiation of adipocytes. Altogether, our study identified CXCL5 as a novel adipokine involved in adipocyte differentiation and acts as an important factor in regulating fat metabolism. We observed the difference between WT and whole-body *Cxcl5* KO in adipose tissue and performed the present study targeting white adipose tissue. To specify the function of CXCL5 in adipose tissue, we isolated SVF cells from adipose tissue from *Cxcl5* KO mice. Therefore, although we generated and used whole-body *Cxcl5* KO mice, we demonstrated the function of CXCL5 in a cell unit. As a future study, it is worthwhile to study the specific role of *Cxcl5* in metabolic-related tissues through tissue-specific KO mouse studies. This study presents a new perspective on treating obesity and metabolic diseases through the understanding of CXCL5 in adipocyte differentiation.

5. Conclusions

This study demonstrated that CXCL5 has an essential role in adipogenesis in adipose tissue. Furthermore, HFD in *Cxcl5* KO mice promoted abnormal adipogenesis and further increased ROS severely. It was explained by showing that the expression of antioxidant enzymes also decreased and failed to remove ROS promptly. Consequently, oxidative stress and insulin resistance have occurred in *Cxcl5* KO mice. These results showed an essential role in the adipogenesis and ROS regulation of CXCL5 in adipose tissue, further suggesting that CXCL5 is a valuable chemokine for metabolic disease research.

Author contributions

D.L. performed and designed most of the experiments, performed the data analysis, and wrote the draft of the manuscript; J.Y.C., K.H.L., and D.W.K. conceived and provided scientific discussion for the study; S.H.Y. performed the animal experiments; and J.Y.C. supervised the project and revised the manuscript. All authors reviewed the manuscript.

Declaration of competing interest

The authors declare that they have no known competing financial interests or personal relationships that could have appeared to influence the work reported in this paper.

Appendix A. Supplementary data

Supplementary data to this article can be found online at https://doi.org/10.1016/j.redox.2022.102359.

References

[1] T.A. Lakka, D.E. Laaksonen, H.-M. Lakka, N. Männikkö, L.K. Niskanen, R. Rauramma, et al., Sedentary lifestyle, poor cardiorespiratory fitness, and the metabolic syndrome, Med. Sci. Sports Exerc. (2003) 1279–1286.
[2] S. Devaraj, J. Wang-Polagruto, J. Polagruto, C.L. Keen, I. Jialal, High-fat, energy-dense, fast-food–style breakfast results in an increase in oxidative stress in metabolic syndrome, Metabolism 57 (2008) 867–870.
[3] P.G. Kopelman, Obesity as a medical problem, Nature 404 (2000) 635–643.
[4] C.N. Lumeng, A.R. Saltiel, Inflammatory links between obesity and metabolic disease, J. Clin. Invest. 121 (2011) 2111–2117.
[5] F.M. Wensveen, S. Valentić, M. Šestan, T.T. Wensveen, B. Polić, Interactions between adipose tissue and the immune system in health and malnutrition, in: Seminars in Immunology, Elsevier, 2015, pp. 322–333.
[6] J. Lu, J. Zhao, H. Meng, X. Zhang, Adipose tissue-resident immune cells in obesity and type 2 diabetes, Front. Immunol. 10 (2019) 1173.
[7] S.S. Pereira, J.I. Alvarez-Leite, Adipokines: biological functions and metabolically healthy obese profile, J. Recept. Ligand Channel Res. 7 (2014) 15–25.
[8] R.B. Harris, Direct and indirect effects of leptin on adipocyte metabolism, Biochim. Biophys. Acta (BBA) - Mol. Basis Dis. 1842 (2014) 414–423.
[9] S.M. Kabir, E.-S. Lee, D.-S. Son, Chemokine network during adipogenesis in 3T3-L1 cells: differential response between growth and proinflammatory factor in preadipocytes vs. adipocytes, Adipocyte 3 (2014) 97–106.
[10] Y. Liu, R. Palanivel, E. Rai, M. Park, T.V. Gabor, M.P. Scheid, et al., Adiponectin stimulates autophagy and reduces oxidative stress to enhance insulin sensitivity during high-fat diet feeding in mice, Diabetes 64 (2015) 36–48.
[11] X. Hui, P. Gu, J. Zhang, T. Nie, Y. Pan, D. Wu, et al., Adiponectin enhances cold-induced browning of subcutaneous adipose tissue via promoting M2 macrophage proliferation, Cell Metabol. 22 (2015) 279–290.
[12] C.L. Sokol, A.D. Luster, The chemokine system in innate immunity, Cold Spring Harbor Perspect. Biol. 7 (2015), a016303.
[13] J. Kusuyama, A. Komorizono, K. Bandow, T. Ohnishi, T. Matsuguchi, CXCL3 positively regulates adipogenic differentiation, J. Lipid Res. 57 (2016) 1806–1820.
[14] D.P. Dyer, J.B. Nebot, C.J. Kelly, L. Medina-Ruiz, F. Schuette, G.J. Graham, The chemokine receptor CXCR2 contributes to murine adipocyte development, J. Leukoc. Biol. 105 (2019) 497–506.
[15] M.-S. Chang, J. McNinch, R. Basu, S. Simonet, Cloning and characterization of the human neutrophil-activating peptide (ENA-78) gene, J. Biol. Chem. 269 (1994) 25277–25282.
[16] T. Persson, N. Monsef, P. Andersson, A. Bjartell, J. Malm, J. Calafat, et al., Expression of the neutrophil-activating CXC chemokine ENA-78/CXCL5 by human eosinophils, Clin. Exp. Allergy 33 (2003) 531–537.
[17] D. Lee, D.W. Kim, S. Yoon, A.-R. Nam, K.-H. Lee, K.-H. Nam, et al., CXCL5 secreted from macrophages during cold exposure mediates white adipose tissue browning, J. Lipid Res. (2021) 62.

[18] J.R. Wisniewski, A. Zougman, M. Mann, Combination of FASP and StageTip-based fractionation allows in-depth analysis of the hippocampal membrane proteome, J. Proteome Res. 8 (2009) 5674–5678.

[19] E.N. Olson, A. Nordheim, Linking actin dynamics and gene transcription to drive cellular motile functions, Nat. Rev. Mol. Cell Biol. 11 (2010) 353–365.

[20] M. Rosenwald, V. Efthymiou, L. Opitz, C. Wolfrum, SRF and MKL1 independently inhibit brown adipogenesis, PLoS One 12 (2017), e0170643.

[21] R. Liu, X. Xiong, D. Nam, V. Yechoor, K. Ma, SRF-MRTF signaling suppresses brown adipocyte development by modulating TGF-β/BMP pathway, Mol. Cell. Endocrinol. 515 (2020), 110920.

[22] J.P. Castro, T. Grune, B. Speckmann, The two faces of reactive oxygen species (ROS) in adipocyte function and dysfunction, Biol. Chem. 397 (2016) 709–724.

[23] S.-J. Park, J.-H. Kim, T-s Kim, S.-R. Lee, J.-W. Park, S. Lee, et al., Peroxiredoxin 2 regulates PGF2α-induced corpus luteum regression in mice by inhibiting ROS-dependent JNK activation, Free Radic. Biol. Med. 108 (2017) 44–55.

[24] Y. Zhou, L. Wang, C. Wang, Y. Wu, D. Chen, T.H. Lee, Potential implications of hydrogen peroxide in the pathogenesis and therapeutic strategies of gliomas, Arch Pharm. Res. (Seoul) 43 (2020) 187–203.

[25] E. Seo, H. Kang, H. Choi, W. Choi, H.S. Jun, Reactive oxygen species-induced changes in glucose and lipid metabolism contribute to the accumulation of cholesterol in the liver during aging, Aging Cell 18 (2019), e12895.

[26] B. Bagheri, A. Alikhani, H. Mokhtari, M. Rasouli, The ratio of unesterified/esterified cholesterol is the major determinant of atherogenicity of lipoprotein fractions, Med. Arch. 72 (2018) 103.

[27] A.L. Ghaben, P.E. Scherer, Adipogenesis and metabolic health, Nat. Rev. Mol. Cell Biol. 20 (2019) 242–258.

[28] C. Chavey, G. Lazennec, S. Lagarrigue, C. Clapé, I. Iankova, J. Teyssier, et al., CXC ligand 5 is an adipose-tissue derived factor that links obesity to insulin resistance, Cell Metabol. 9 (2009) 339–349.

[29] M. Higurashi, Y. Ohya, K. Joh, M. Muraguchi, M. Nishimura, H. Terawaki, et al., Increased urinary levels of CXCL5, CXCL8 and CXCL9 in patients with Type 2 diabetic nephropathy, J. Diabetes Complicat. 23 (2009) 178–184.

[30] C.S. Nunemaker, H.G. Chung, G.M. Verrilli, K.L. Corbin, A. Upadhye, P.R. Sharma, Increased serum CXCL1 and CXCL5 are linked to obesity, hyperglycemia, and impaired islet function, J. Endocrinol. 222 (2014) 267–276.

[31] Y. Sun, Y. Lu, J. Saredy, X. Wang, I.V.C. Drummer, Y. Shao, et al., ROS systems are a new integrated network for sensing homeostasis and alarming stresses in organelle metabolic processes, Redox Biol. (2020), 101696.

[32] X. Wang, Redox Modulation of Adipogenesis. Redox-Principles and Advanced Applications, IntechOpen, 2017.

[33] Z. Chen, R. Tian, Z. She, J. Cai, H. Li, Role of oxidative stress in the pathogenesis of nonalcoholic fatty liver disease, Free Radic. Biol. Med. 152 (2020) 116–141.

[34] M. Jastroch, Uncoupling protein 1 controls reactive oxygen species in brown adipose tissue, Proc. Natl. Acad. Sci. Unit. States Am. 114 (2017) 7744–7746.

[35] H. Lee, Y.J. Lee, H. Choi, E.H. Ko, J-w Kim, Reactive oxygen species facilitate adipocyte differentiation by accelerating mitotic clonal expansion, J. Biol. Chem. 284 (2009) 10601–10609.